THREE-DIMENSIONAL MODELING OF ALONGSHORE CURRENT DYNAMICS

Kristen D. Splinter and Donald N. Slinn
Department of Civil and Coastal Engineering, University of Florida
Gainesville, Florida 32611-6590 USA

ABSTRACT

The time-dependent behavior of low frequency alongshore currents produced by obliquely incident waves in the surf zone is examined using a non-hydrostatic, phase-averaged, three-dimensional (3-D) numerical model. The model employs alongshore uniform barred beach topography and invokes periodicity in the alongshore direction. It solves the Navier-Stokes equations with a Large Eddy Simulation (LES) sub-grid scale closure model on a curvilinear (σ-coordinate) grid. Simulations of alongshore currents are forced using two cross-shore distributions of momentum input. In preliminary cases a Gaussian cross-shore distribution is specified. In subsequent model runs, the alongshore and cross-shore momentum inputs are specified using an empirical wave breaking sub-model (Thornton and Guza, 1983, 1986) that calculates the radiation stress gradients from the shoaling wave field. Additional complexity, compared to depth averaged models, is introduced in the three-dimensional model because the distribution of momentum input to the model must also be specified as a function of depth. In order to examine the sensitivity to this approximation, we investigate the modeled alongshore current response for depth uniform and depth dependent distributions of the forcing. Depth uniform forcing in the 3-D model produces alongshore current response qualitatively similar to what is produced in traditional depth integrated (2-D) models. The low-frequency currents become unstable to shear instabilities with alongshore wavelengths of order 100 m and periods of 100 s. Depth dependent forcing, however, produces very different features in the alongshore currents. A shoreward mass flux in the top half of the water column and strong compensating undertow are present in the 3-D simulations. When the alongshore current decays with depth, the cross-shore circulation has the net effect of shifting the alongshore current maximum from over the location of the sand bar into the trough. A second feature of the depth dependent structure is that vertical shear instabilities induce large amplitude perturbations to the mean alongshore current and it destabilizes much more rapidly and breaks down into a turbulent flow with higher frequency statistics than produced with depth uniform forcing. The results presented here are considered preliminary, various model approximations are being evaluated and the simulations have not yet been run out to steady state conditions so the results are tentative, pending further study and comparison with field and laboratory measurements.

INTRODUCTION

Strong alongshore currents on the order of 1 m/s are generated in the nearshore region by the alongshore component of the momentum flux from obliquely incident breaking surface waves (Longuet-Higgins, 1970). Most contemporary nearshore circulation models (e.g., Allen et al., 1996; Slinn et al, 1998, 2000; Ozkan and Kirby, 1999; Van Dongeren and Svendsen, 2000; Reniers et al., 2003) have used some form of the two-dimensional (2-D) depth-integrated flow approximation. This is a reasonable assumption, since the water depth is shallow, O(1m) compared to its characteristic horizontal length scales, O(100m). The nearshore region, however, has several salient three-dimensional (3-D) features that the 2-D approximation obscures that may be important in determining the strength and location of the alongshore currents. One of these is that shoreward mass flux and cross-shore momentum input into the water column from shoaling waves localized in the upper portion of the water column is balanced by an offshore return flow known as the undertow. The resulting cross-shore circulation may then act to diffuse the alongshore current horizontally and decrease the shear and strength of the alongshore current.

The focus of our numerical experiments is to determine the role of these processes by modeling 3-D nearshore circulation including the dynamics of the undertow. We find that the presence of the undertow has order-one effect on both the mean alongshore currents and the shear instabilities of the time-averaged statistics of the unsteady flows. Field observations at Duck, North Carolina by Oltman-Shay et al. (1989) have shown the presence of alongshore propagating disturbances associated with alongshore currents. These motions have different characteristics than surface gravity waves because their wave periods, O(100 s), are too long in comparison to their wave length, O(100 m). Bowen and Holman (1989) used linear stability analysis to show that these disturbances could be caused by the cross-shore shear of depth-averaged alongshore currents. Our simulations draw attention to two interesting results. First, we find that the 3-D flows are more unstable than produced by depth integrated models. Second, we find that the dynamics of the undertow and cross-shore circulation produce a peak alongshore current in the trough, without the need to include a surface roller model, in cases where the waves break over a sand bar, similar to situations observed during the DELILAH field experiment. (Church & Thornton, 1993)

MODEL

Our Computational Fluid Dynamics (CFD) model is a 3-D Large-Eddy Simulation (LES) nearshore circulation model implementing the Smagorinsky sub-grid scale closure scheme. It models the wave-phase-averaged, time-dependent, low-frequency currents, in a curvilinear, bottom conforming, σ-coordinate system, with a rigid, free-slip lid at the surface (Winters et al, 2000). Bottom stress is included with a no-slip condition at the bottom boundary and resolved through the use of a vertically clustered grid. The model is periodic in the alongshore direction, with a shore parallel sand bar located approximately

80 meters from the shoreline. The grid resolves centimeter scales near the seabed, adequate for the LES turbulence closure scheme to produce realistic time-averaged vertical velocity profiles. The effect of alternate sub-grid scale dissipation models is a topic of ongoing investigation.

Grid Metrics and Transformation

Figure 1 illustrates the problem geometry and grid coordinate system used in the model. The physical domain is 200 m x 198 m in the *x*-*y* direction, reaching a depth of 4.5 m at the offshore boundary following a depth profile approximate to topography measured at Duck, North Carolina, October 11, 1990, as part of the DELILAH field experiment (Lippmann et al., 1999). The beach topography has alongshore-uniform bathymetry and includes a distinct shore-parallel alongshore bar–trough system. The computational domain is composed of 129 x 129 x 33 (549,153 total) grid points. The grid is clustered in both the vertical and horizontal directions with additional grid resources deployed near the shoreward boundary and the seabed. The grid spacing is on the order of 1 meter horizontally, and 10 centimeters vertically, decreasing in the vertical near the seabed.

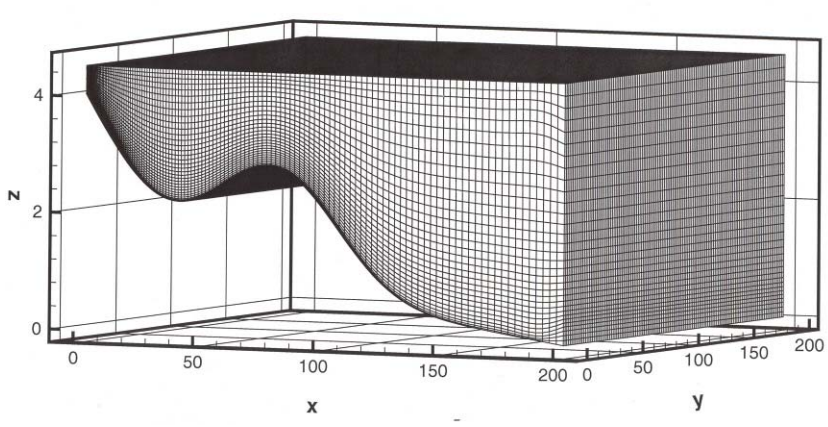

Figure 1: Physical grid layout used in numerical simulations to represent the beach profile at Duck, North Carolina, October 11, 1990, as part of the DELILAH field experiment (Lippmann et al., 1999).

In order to compute approximate solutions to the governing equations, the physical domain (*x, y, z*) in Figure 1 is transformed to a cubic grid of regularly spaced grid points in computational space (ξ,η,ζ). The model uses a uniform grid, with constant spacing of approximately 1.5 m in the *y*-direction. The mapping between physical and computational space is done through an orthogonal transformation of three successive elliptic boundary value problems following Winters et al. (2000).

Forcing

The momentum input due to breaking waves is included through a steady 3-D body force. We present results from four cases. We examine two cross-shore distributions of the momentum input, and for each, implemented separately, depth uniform and depth-dependent forcing. First we implement a Gaussian cross-shore distribution of momentum. The magnitude of the forcing is set by experimentation to produce alongshore currents of O(1 m/s): $G(x) = -0.005 * \exp\left(-\frac{(x-x_0)^2}{\alpha^2}\right)$, where x is the cross-shore position, x_0 = 80 m is the location of the peak momentum input (co-located with the crest of the sand bar), and α = 0.1, controls the width of the Gaussian distribution. The forcing is inputted into both the x- and y-momentum equations, with the relative magnitudes determined by a specified shoaling wave angle ($G(x)\cos\theta$, $G(x)\sin\theta$). The second cross-shore distribution of momentum input is determined by coupling a shoaling wave field to the bottom topography (Slinn et al, 1998) with a wave refraction model, including the wave-breaking dissipation sub-model of Thornton and Guza (1983) and calculating the resulting radiation stress gradients in the x- and y-directions. The forcing is either distributed uniformly in the vertical or linearly distributed with depth, i.e., $G(x,z) = G(x)(z - z_0)$, where z_0 is the local bottom depth following the recommendations by Fredsoe and Deigaard (1992, Eqn. 6.17). Figure 2 displays the cross-shore distribution of the total momentum forcing applied to the model for the experiments.

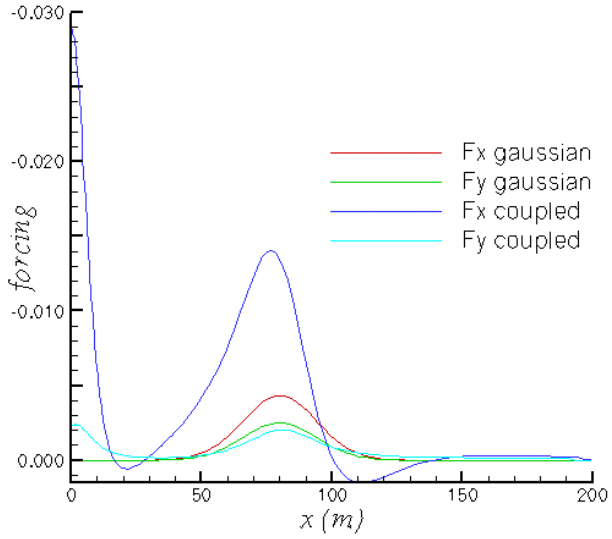

Figure 2: Cross-shore distributions of the x- and y- components of the non-dimensional momentum forcing for the model experiments. Cases 1 and 2 were conducted with the Gaussian forcing and Cases 3 and 4 used the radiation stress gradients calculated with the wave-shoaling model.

Governing Equations

The LES equations for 3-D, unsteady, incompressible flow with forcing are:

$$\frac{\partial u_i}{\partial t} + u_j \frac{\partial u_i}{\partial x_j} = -\frac{1}{\rho}\frac{\partial p}{\partial x_i} + \frac{\partial \tau_{ij}}{\partial x_i} + F^{(x_i)} \qquad (1)$$

$$\frac{\partial u_i}{\partial x_i} = 0\,, \qquad (2)$$

where $u_i = (u, v, w)$ are the cross-shore, alongshore and vertical velocity components, p is pressure, t is time, ρ is fluid density, and $F^{(x)}$ and $F^{(y)}$ are the horizontal body forces in the cross-shore and alongshore directions. $\tau_{ij} \equiv \overline{u_i u_j} - \overline{u}_i \overline{u}_j$ represents the LES sub-grid stresses written in terms of the resolved strain tensor, *e.g.,* $\tau_{ij} - \frac{\delta_{ij}}{3} \equiv -2\nu_t \overline{S}_{ij}$ where $\overline{S}_{ij} \equiv \frac{1}{2}\left(\frac{\partial u_i}{\partial x_j} + \frac{\partial u_j}{\partial x_i}\right)$ and the turbulent eddy viscosity, ν_t , is calculated with the Smagorinsky approach, i.e., $\nu_t = \left(C\overline{\Delta}\right)^2 \left(2\overline{S}_{ij}\overline{S}_{ij}\right)^{1/2}$, where $C = \pi^{-1}\left(\frac{2}{3}C_k\right)^{3/4}$ and $C_k = 1.5$ is the Kolmogorov constant and $\overline{\Delta} = (\Delta_x \Delta_y \Delta_z)^{1/3}$ is the filter width based on the local grid spacing in each direction. We have implemented a no-slip condition at the shoreward (truncated domain) boundary, and a no-slip boundary condition at the offshore boundary. A fourth order-compact low pass filter (Lele, 1992) is also applied to the velocity field to help maintain a resolved and stable simulation. The reader is referred to Winters et al. (2000) for a more detailed description of the model. We note there are two of the most potentially limiting approximations in our model compared to the physics that may occur in the associated physical problem in nature. First is the application of the LES model on the anisotropic grid (Scotti, et al. 1997). The second is that we apply wave forcing over the mean water column, whereas a significant portion of breaking wave events occur above the mean water level, and therefore presumably the approximation we have chosen for depth dependent forcing is flawed. These approximations, however, are rational exploratory steps forward from 2-D modeling approaches and produce results that may increase insight into nearshore circulation.

NUMERICAL EXPERIMENTS

We report on results from 4 cases. Case 1 (C1) is the depth uniform Gaussian case. Case 2 (C2) uses the depth dependent Gaussian forcing. Case 3 (C3) is the depth uniform Thornton-Guza (T-G) experiment. Case 4 (C4) uses the depth dependent T-G forcing. The offshore wave angle for Cases 3 and 4 was 30°. Additional cases with different offshore wave angles were also conducted that support the conclusions from the experiments presented here. The primary consequence of varying the incident wave angle

is to modify the relative magnitudes of the cross-shore and alongshore radiation stress gradients and to adjust the relative strength of the cross-shore circulation and alongshore current.

RESULTS

The four numerical experiments produce different predictions of the alongshore current profiles, stability, and vertical structure. We present contours of the alongshore surface currents, *v(x,y,t),* for Cases 1 and 2 during times of flow development in Figure 3. The first major difference between depth uniform (C1) and depth dependent (C2) forcing is that instabilities of the alongshore current develop much sooner with the depth dependent flow. The second major difference is that the strength that the surface current (and depth averaged current) achieves is much stronger before breaking down into instability and turbulence in the case of depth uniform forcing. The third significant difference between the flow development is that the alongshore wavelength of the initial instabilities are much longer (of order 100's of meters) for the depth uniform current, but on the order of 10's of meters for the depth dependent current. The fourth interesting flow feature is that the peak alongshore current moves outside of the sand bar for the depth uniform current after the flow becomes unstable, but it moves inside the sand bar, into the trough for the depth dependent forcing.

Clearly there are very significant implications for the behavior of the alongshore current depending on the depth dependence of the forcing. We note that the behavior in the simulation with depth uniform forcing case is qualitatively similar to the flow development that we have observed in previous numerical experiments with depth-averaged models (Slinn et al, 1998, 2000). The distinctive features observed here for the depth dependent forcing: rapid instability of the alongshore current, small-scale instabilities, and the shoreward shift of the peak current are entirely new. The most interesting aspect of these new observations are that they may have a very logical, and previously neglected explanation (discussed below), and that the shoreward shift of the peak alongshore current is similar to puzzling phenomenon that has been observed in nature (Church & Thornton, 1993).

The surface currents for Cases 3 and 4 are shown during initial periods of flow development in Figure 4. The same contrasting flow features are also apparent for the coupled T-G wave forcing. The currents with depth dependent forcing, 1) break down sooner, 2) develop smaller scale features, 3) diffuse more in the cross-shore direction, and 4) shift the current maxima into the trough. Again, the 2-D depth averaged models produce results much more qualitatively similar to the 3-D simulation with depth uniform forcing. We contend that the depth dependent forcing more closely resembles the situation in most natural beach situations, and that the newly modeled behavior in the 3-D model observed in Cases 2 and 4 is a more consistent approximation of nearshore current

behavior. Insight into the dynamics that produce the different cross-shore distributions of the alongshore currents is gained by examining Figure 5 and Figure 6 below.

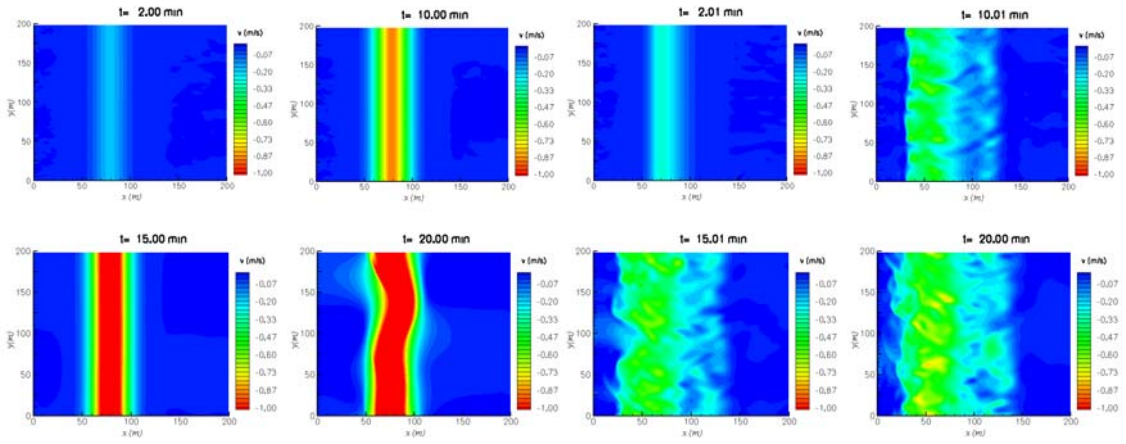

Figure 3: x-y plots of the surface alongshore velocity field for Cases 1 (two left columns) and 2 (two right columns) during phases of flow development. The wave direction is 30^o. For the depth uniform forcing the current remains more organized and centered over the bar, located at x = 80 m, producing currents over 1 m/s and by t = 20 min, long wavelength instabilities are developing. For depth dependent forcing, the flow destabilizes into smaller scale motions more rapidly, diffuses horizontally, and the peak currents of approximately 0.5 m/s drifts shoreward of the bar crest.

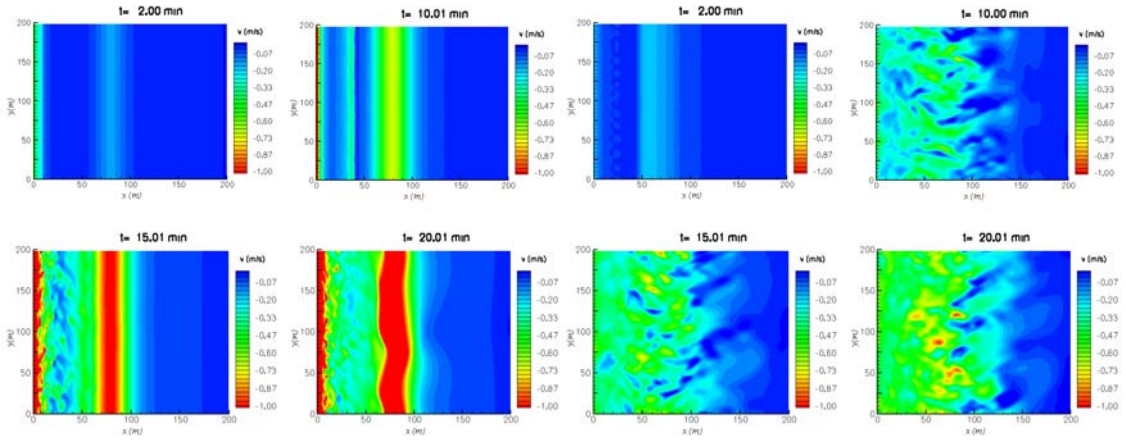

Figure 4: x-y plots of the surface alongshore velocity field for Cases 3 (two left columns) and 4 (two right columns) during phases of flow development. The offshore wave direction is 30^o. For the depth uniform forcing the current remains more organized and centered over the bar, located at x = 80 m, producing currents over 1 m/s and by t = 20min, long wavelength instabilities are developing. For depth dependent forcing, the flow destabilizes into smaller scale motions more rapidly, diffuses horizontally, and the peak currents of approximately 0.5 m/s drifts shoreward of the bar crest.

The cross-shore and depth distribution of the alongshore velocity profiles reveal effects of 3-D mixing and preferential cross-shore advection. It appears that the physical

explanation has two major components. The first is that much stronger cross-shore circulation develops for the depth dependent forcing. When $F^{(x)}$ is depth uniform, little cross-shore circulation is produced, rather, a barotropic cross-shore pressure gradient balances the forcing. When $F^{(x)}$ is depth dependent, a strong undertow develops rapidly, compensated by a shoreward mass flux in the top half of the water column. The reason this is dynamically important to the depth averaged alongshore current is that $F^{(y)}$ is also depth dependent and there is a much stronger alongshore current in the top half of the water column than in the bottom. Thus the faster near surface alongshore current is advected shoreward (into the trough) while the weaker bottom alongshore current drifts offshore. The net effect is a shoreward shift of the alongshore current maxima. Interestingly, in the examples we have investigated, the depth-averaged maxima becomes balanced in the trough.

The net effect of this cross-shore dispersion on the mean alongshore current is similar to including a roller model to the shoaling surface wave sub-model in order to shift the location of wave momentum input shoreward. We have not included a roller model in the formulations of the T-G model that we have implemented here. Alternate hypotheses have been set forward previously to explain current maxima in the trough. A leading candidate is the effect of topographically coupled alongshore pressure gradients (Slinn, et al., 2000). We have no mean alongshore pressure gradients in this model because the bathymetry is alongshore uniform, and we use steady forcing without wave-current interaction (Yu & Slinn, 2003).

Complementary lines of investigation have considered net effects of the undertow on depth-averaged currents, such as the formulations in the quasi-3D implementation of Shorecirc (*e.g.,* Putrevu and Svendsen, 1999). They have not observed current behavior qualitatively similar to what we see here. It appears that the reason is that in their formulation, they use the quasi-3D information primarily to estimate an isotropic horizontal diffusion coefficient. This would be an excellent approximation if the alongshore current were depth uniform because the shoreward mass flux in the top half of the water column would carry equal amounts of alongshore momentum as the undertow carries offshore. Perhaps this would be the best approximation for plunging breakers that vigorously stirred the water column at high frequency, or if the bottom boundary layer of the alongshore current was very thin. If, however, the alongshore current is depth dependent, either because the momentum input is depth dependent, or because bottom friction develops a thick boundary layer, then it is reasonable that the net effect of three-dimensional cross-shore circulation would be to produce, non-isotropic, preferentially shoreward diffusion of the alongshore currents.

Figure 5 shows the alongshore currents in a vertical cross-section of the flow during flow development for Cases 1 and 2. In Case 2 (right panels), the signature of the undertow can be seen by offshore drift of alongshore momentum near the seabed. The circulation cells also produce mixing in the vertical direction as unstable vortices (ω_y) develop, that pull surface water downward, decreasing surface alongshore velocities and spreading the

alongshore current laterally. At these early times (left panels), Case 1, with depth uniform forcing, has little cross-shore or vertical variability of the alongshore current. A bottom boundary layer is developing, due to the no-slip boundary condition.

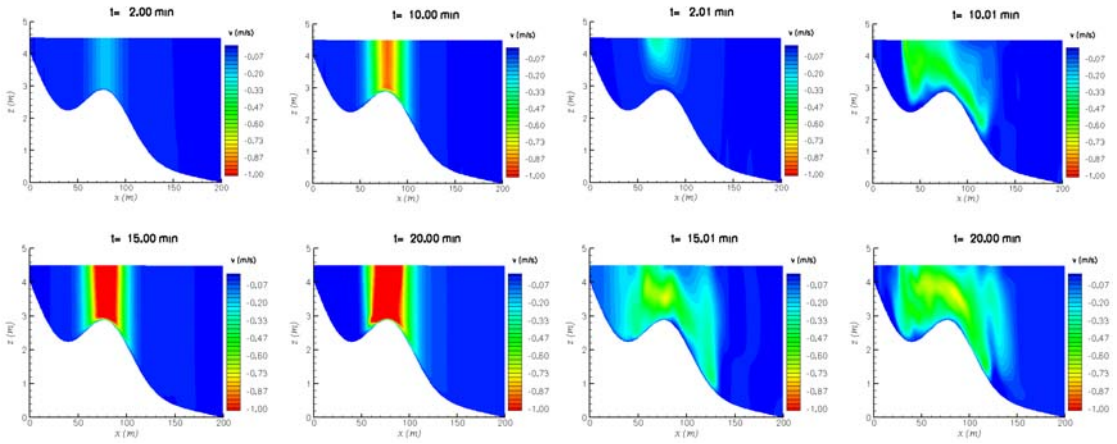

Figure 5: x-z contour plot of alongshore velocity at y = 99 m for Cases 1 and 2 at t = 2, 10, 15, and 20 min. Wave direction is 30 degrees. Migration of the mean current can be seen in the time series as well as the undertow, indicated by the blue region (v = 0 m/s) along the bottom topography. The undertow is not as predominant in the uniform forcing and alongshore current migration shoreward is minimized with minimal lateral spreading as velocities increase.

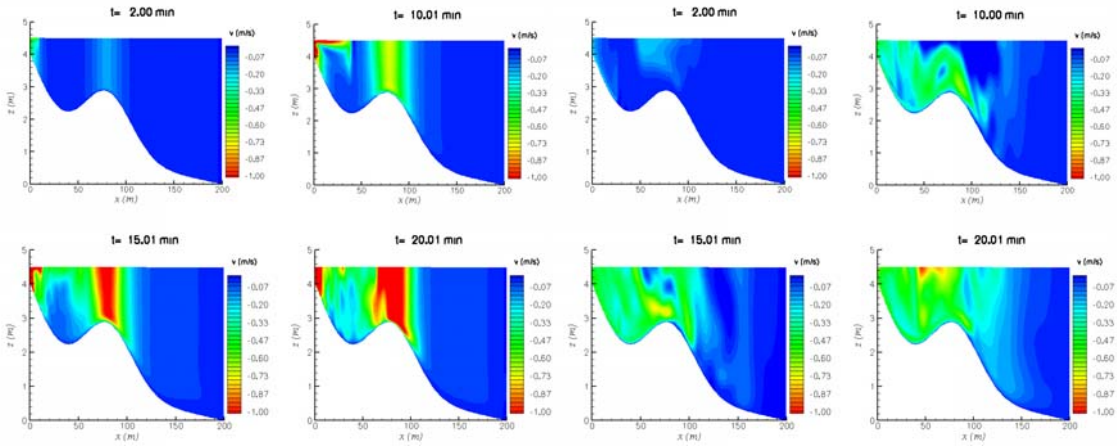

Figure 6: x-z contour plot of alongshore velocity at y = 99 m for Cases 3 and 4. In Case 4 (right panels) the alongshore current generated at the shoreline is pulled seaward from the undertow which can be seen at t = 10 min. The current is milder than in Case 1 or 2 and encompasses more cross-shore area between the bar and the shoreline due to mixing between the 2 areas of concentrated forcing.

In Cases 3 and 4 qualitatively similar results are obtained (Figure 6). The depth uniform current over the sand bar stays in place much longer and has different alongshore

instability properties. More information on the time dependent mean flow development is available in Figure 7 and Figure *8* below.

A curious feature is observed at early times for the depth uniform flow for which we have not yet found an adequate explanation. The coupled T-G forcing produces 2 alongshore current maxima, one at the shoreline, and one located over the bar. Over time, the 2 profiles both migrate towards the trough area. At early time a surface current, apparently from a secondary circulation, or an instability of the nearshore jet, diffuses offshore. It is possible that the secondary circulation is influenced by the interaction of the barotropic cross-shore pressure gradient and the no-slip bottom boundary condition that may have more pronounced effect in the shallow water near the shore.

The cross-shore distribution of the depth- and alongshore-averaged alongshore velocity profiles are shown in Figure 7 (Gaussian forcing) and Figure 8 (T-G coupled forcing) during times of flow development. For Case 1 after approximately t = 20 min the flow destabilizes and the current maxima shifts offshore of the sand bar. The turbulence intensifies and eventually produces a mean alongshore current with a peak velocity of approximately 50 cm/s. In this case, it is unfortunate that we used a no-slip boundary condition at x = 200 m at later times, but we expect that repeating the simulation with a free-slip condition would yield substantially similar results. We also intend to test a wider model domain out to x = 300 m. Case 2, with depth dependent forcing, also eventually produces a maximum current of approximately 50 cm/s. The maxima initially migrates shoreward and eventually rests close to x = 80 m rather than shifting offshore of the sandbar. It appears that there is a balance in this case of offshore diffusion by turbulent eddies into deeper water and shoreward diffusion by the mean cross-shore circulation so that the peak current at later times is close to the peak of momentum input. The shoreward diffusion by cross-shore circulation is absent from Case 1, and in that case the peak current shifts offshore.

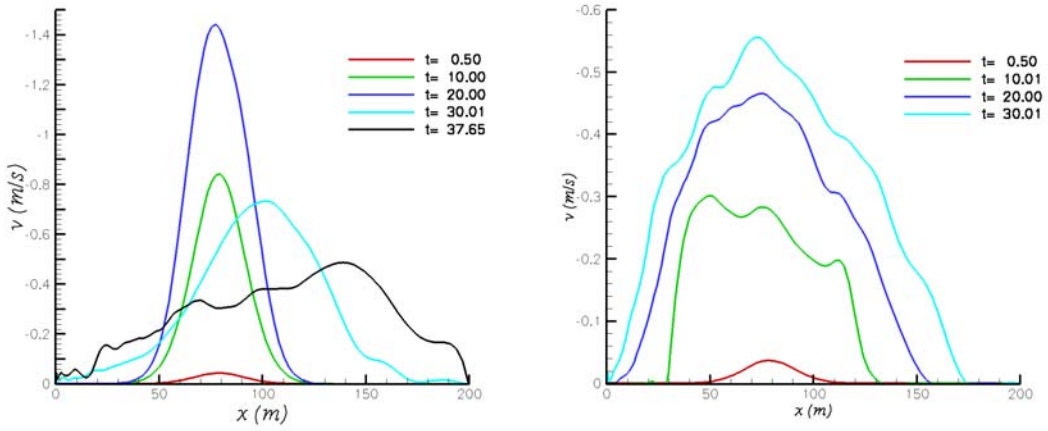

Figure 7: Alongshore and depth-averaged alongshore velocity profiles for Cases 1 and 2 during times of flow development.

Figure 8 shows the cross-shore distribution of the depth- and alongshore-averaged alongshore velocity profiles for Cases 3 and 4 during times of flow development. In Case 3, after the flow becomes turbulent, around t = 25 min, the alongshore current spreads into the trough, but a local maxima persists over the sand bar, near x = 70 m, with a velocity near 75 cm/s. In Case 4 (right panel) the peak current has shifted to near x = 60 m and the shoreline jet is much weaker. An approximate steady state has been achieved for t ≥ 40 min, though the offshore turbulent diffusion is continuing to strengthen the current for x > 150 m. We intend to run these simulations out to later times to verify our preliminary conclusions.

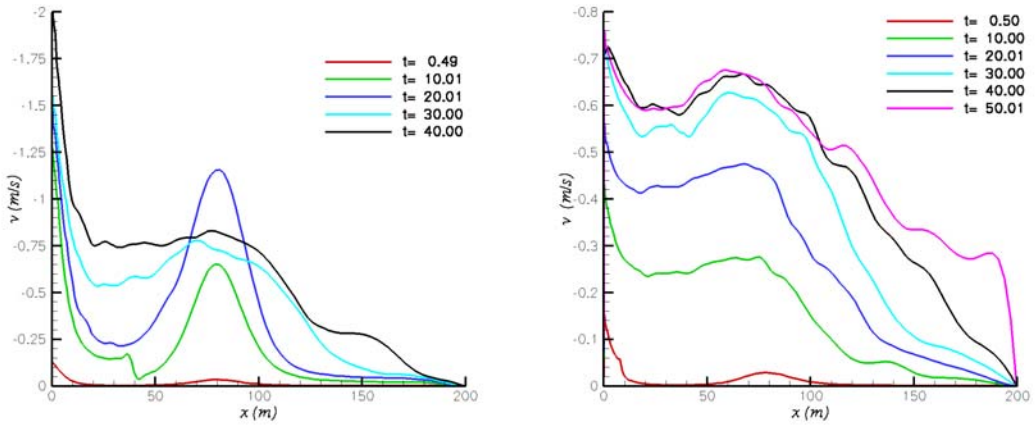

Figure 8: Alongshore and depth-averaged alongshore velocity profiles for Cases 3 and 4.

Figure 9 and Figure *10* show the alongshore-averaged cross-shore circulation for the numerical experiments. A reference vector is shown that represents velocities of 1 m/s. We note that the scales between the depth uniform forcing experiments (left panels) and the depth dependent forcing cases are significantly different. They are shown in this manner to illustrate that some depth dependent cross-shore structure develops in the depth uniform experiments, but that it may be especially prominent in the bottom boundary layer (Case 1) and in shallower water near the shoreline (Case 3). The clearest feature in both Figure 9 and Figure 10 is the signature of the undertow and the compensating shoreward flow in the upper portion of the water column for the cases with depth dependent forcing in the right panels.

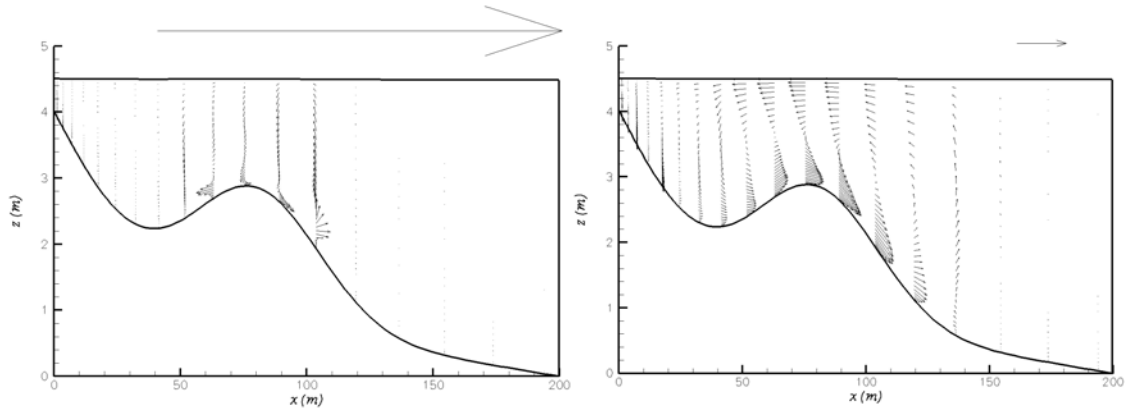

Figure 9: Alongshore averaged, u-w velocity vectors at t = 20 min for Cases 1 and 2.

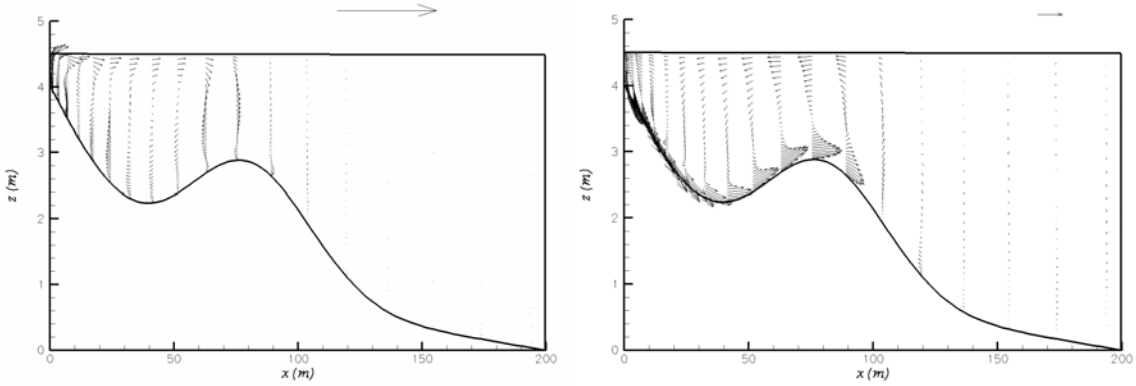

Figure 10: Alongshore averaged u-w velocity vectors at t = 20 min for Cases 3 and 4.

SUMMARY

We have implemented a new three-dimensional nearshore circulation model to examine alongshore currents over barred beach topography. We have forced the model with depth uniform and depth dependent momentum input. The alongshore currents that develop are strongly dependent on the forcing. An important dynamic appears to be that the induced cross-shore circulation causes relatively faster moving surface alongshore currents to be advected shoreward compared to the slower bottom currents that are displaced offshore by the undertow. The cross-shore circulation also influences the destabilization of the alongshore currents and causes them to break into turbulence faster and into smaller horizontal structures than produced by depth-uniform forcing conditions or in depth-averaged models. A particularly interesting feature of the model experiments is the shifting of the alongshore current maxima into the trough without the use of a roller model or alongshore pressure gradients. This work is preliminary and the conclusions are tentative. However, it appears that 3-D modeling will be able to add an interesting new

dimension to our theoretical understanding of nearshore circulation and to the non-linear time dependent dynamics of low frequency motions in the surf zone.

FUTURE WORK

Our ongoing research is focusing on further model development and analysis of the flow fields to obtain more realistic information about alongshore and cross-shore velocity profiles, and the development of the instabilities. We are attempting to repeat our experiments at higher grid resolution and with different horizontal domain sizes to demonstrate the independence of our results from model approximations and constraints of computational resources. We intend to compare our 3-D results directly to similar 2-D model predictions and available field data. Since a primary result of this work is that the alongshore currents depend sensitively on the choice of the depth dependent forcing, we are also attempting to assess how the vertical distributions depend on wave conditions.

ACKNOWLEDGEMENTS

We would like to thank Kraig Winters, Brian Barr, and Jamie MacMahan for their assistance. This work is supported by the National Science Foundation under a grant from the Physical Oceanography directorate through the CAREER Award program.

REFERENCES

Allen, J.S., Newberger, P.A., and Holman, R., 1996. Nonlinear shear instabilities of alongshore currents on plane beaches. *Journal of Fluid Mechanics*, **310**, 181-213.

Bowen A.J., and Holman, R.A., 1989. Shear Instabilities of the Mean Longshore-Current 1. Theory. *Journal of Geophysical Research-Ocean.***94 (C12)**: 18023-18030.

Church, J.C., Thornton, E.B. 1993. Effects of breaking wave induced turbulence within a longshore current model. *Coastal Engineering,***20**, 1-28.

Feddersen, F., Guza, R.T., Elgar, S., and Herbers, T.H.C. 1998. Alongshore momentum balances in the Nearshore, *Journal of Geophysical Research*, **103**, 15,667-15,676.

Fredsoe, J. and Deigaard, R., 1992. *Mechanics of Coastal Sediment Transport*, World Scientific, 369 pp.

Lele, S. K., 1992. Compact finite difference schemes with spectral-like resolution. *Journal of Computational Physics*, 103, 16-42.

Lippmann, T.C., Herbers, T.H.C., and Thornton, E.B., 1999. Gravity and shear wave contributions to nearshore infragravity motions. *Journal of Physical Oceanography*. **29**, 231-239.

Longuet-Higgins, M.S., 1970. Longshore Currents Generated by Obliquely Incident Sea Waves, 1. *Journal of Geophysical Research*., **75**, 6778-6789.

Ozkan-Haller, H.T., and Kirby, J. T. 1999. Nonlinear evolution of shear instabilities of the longshore current: A comparison of observations and computations. *Journal of Geophysical Research*, **104**, 25953-25984.

Oltman-Shay, J., Howd, P.A., and Birkemeier, W.A., 1989. Shear instabilities of the mean Longshore current, 2. Field data, *Journal of Geophysical Research*, **94**: 18031-18042.

Putrevu, U., Svendsen, I.A., 1999, Three-dimensional dispersion of momentum in wave-induced nearshore currents, *European Journal of Mechanics, B, Fluids,* 409-427.

Reniers, AJ.H.M., Thornton, E.B., Lippmann, T.C., Battjes, J.A., 2003. Effects of Alongshore Non-uniformities on Longshore Currents Measured during Delilah. Submitted to the *Journal of Geophysical Research*.

Scotti, A., Meneveau, C., Fatica, M.. 1997. Dynamic Smagorinsky model on anisotropic grid. *Physics of Fluids*, **9**, 1856-1858.

Slinn, D.N., Allen, J.S., Newberger, P.A., Holman, R.A., 1998. Nonlinear shear instabilities of alongshore currents over barred beaches. *Journal of Geophysical Research*, **103**, 18357-18379.

Slinn, D.N., Allen, J.S., Holman, R.A. 2000. Alongshore currents over variable beach topography. *Journal of Geophysical Research*, **105**, 16971-16998.

Thornton, E.B. and Guza, R.T. 1983. Transformation of wave height distribution. *Journal of Geophysical Research,* **88.** 5929-5938.

Thornton, E.B. and Guza, R.T. 1986. Surf zone longshore currents and random waves: Field data and models. *Journal of Physical Oceanography,* **16**, 1165-1178.

Yu, J. and Slinn, D. N. 2003. Effects of wave-current interaction on rip currents. *Journal of Geophysical Research*, **108**, C3, 3088, doi:10.1029/2001JC001105.

Van Dongeren, A.R., and Svendsen, I.A., 2000. Nonlinear and quasi 3-D effects in leaky infragravity waves. *Coastal Engineering*, **41**,4, pp.467-496.

Winters, K.B., Seim, H.E., and Finnigan, T.D., 2000. Simulation of non-hydrostatic, density-stratified flow in irregular domains. *Int. J. Numer. Meth. Fluids*. **32**:263-284.